Struct Multidisc Optim 22, 12–23 © Springer-Verlag 2001

# Analysis and optimization of energy flows in structures composed of beam elements – Part II: examples and discussion

**S.V. Sorokin, J.B. Nielsen and N. Olhoff**

**Abstract** This paper addresses analysis and optimization of in-plane coupled flexural and longitudinal vibrations within the framework of a theory outlined in a companion paper. An optimization problem is posed for a model structure consisting of two elements of a finite length and one semi-infinite element. This model structure has four terminal points. Parameters of design are chosen as stiffness, mass and the location of two of the terminal points. A parametric study of vibrations of the structure is performed and optimal locations of terminal points are detected. Analysis of energy flows between elementary dynamical systems is done and the dynamics of a structure with the optimized design shape is compared with the dynamics associated with the initial design shape. The formulation of the optimization problem is also extended to include amplitudes of "secondary forces" as design variables. Possibilities of active control of energy flows by usage of "secondary" sources of excitation are discussed.

**Key words** elastic beam structures, power flow, minimization of emitted or transmitted energy of vibrations, dynamical subsystems, substructuring, wave guides, boundary equations

## 1 Introduction

In Part 1 of this paper, a theory of analysis of in-plane coupled flexural and longitudinal vibrations of a planar structure composed by tubular elements of both a finite and an infinite length is presented. The mechanical system is modelled by a set of coupled subsystems introduced as elastic wave-guides carrying flexural or longitudinal waves. The purpose of the study is an optimization of energy flows from a source to a remote zone of a structure for a given frequency range and given excitation conditions by means of varying the location, stiffness, damping and mass parameters of the attached terminal points. A boundary integral equation method is used to set up a system of governing equations describing forced stationary vibrations of the structure.

In Part 2, validity of this problem formulation is checked via comparison of numerical results obtained by usage of the boundary integral method, the finite element method and the spectral element method. Then a parametric study of vibrations of a model structure is performed and optimization examples are considered.

*Received April 4, 2000*
*Revised manuscript received October 18, 2000*

S.V. Sorokin[1], J.B. Nielsen[2] and N. Olhoff[2]

[1] Department of Engineering Mechanics, State Marine Technical University of St. Petersburg, Lotsmanskaya str. 3, St. Petersburg, 190008, Russia
e-mail: sorokins@mail.ru
[2] Institute of Mechanical Engineering, Aalborg University, Pontoppidanstraede 101, DK-9220 Aalborg East, Denmark
e-mail: no@ime.auc.dk

## 2 Verification of computational algorithm

To check the validity of solutions to the problem obtained by the boundary equation method, analysis of free vibrations of the structure of finite length introduced in the companion paper has been done first. Parameters of the elements of the structure are specified as follows: lengths $\ell_1 = 1\,\mathrm{m}$, $\ell_2 = 0.5\,\mathrm{m}$, $\ell_3 = 3\,\mathrm{m}$, outer diameters $d_1 = d_2 = 0.0275\,\mathrm{m}$, $d_3 = 0.055\,\mathrm{m}$, thickness $t_1 = t_2 = 0.0025\,\mathrm{m}$, $t_3 = 0.005\,\mathrm{m}$, material density $\rho_1 = \rho_2 = \rho_3 = 7800\,\mathrm{kg/m^3}$ and Young's modulus $E_1 = E_2 = E_3 = 2.1 \times 10^{11}\,\mathrm{Pa}$. Two sets of boundary conditions have been considered. For a simply supported structure, boundary conditions (3) and (8) from Part I are formulated as

$$u_1(0) = w''(0) = 0\,,$$

$$u_3(\ell_3) = w_3(\ell_3) = w''(\ell_3) = 0\,.$$

The first five eigenfrequencies found by the standard finite element package ANSYS and via boundary integral equations (BIE) are shown in Table 1.

**Table 1** Eigenfrequencies of a simply supported structure

| | | | | | |
|---|---|---|---|---|---|
| ANSYS | 4.624 Hz | 25.145 Hz | 76.313 Hz | 102.23 Hz | 161.44 Hz |
| BIE | 4.625 Hz | 25.152 Hz | 76.358 Hz | 102.29 Hz | 161.75 Hz |

**Table 2** Eigenfrequencies of a "free-free" structure

| | | | | | |
|---|---|---|---|---|---|
| ANSYS | 14.62 Hz | 34.98 Hz | 49.67 Hz | 96.02 Hz | 145.66 Hz |
| BIE | 14.62 Hz | 35.02 Hz | 49.68 Hz | 96.16 Hz | 145.83 Hz |

For an unconstrained structure, boundary conditions (3) and (8) from Part I are formulated as

$$u_1'(0) = w_1(0) = w'''(0) = w''(0) = 0\,,$$

$$u_3'(\ell_3) = w_3'''(\ell_3) = w''(\ell_3) = 0\,.$$

The first five eigenfrequencies of an unconstrained structure are displayed in Table 2

The difference between eigefrequencies obtained via ANSYS and via BIE is of the same order of magnitude as one proceeds to higher frequencies or to any other boundary conditions.

As has been discussed, the system of boundary integral equations for a structure containing a semi-infinite element is obtained by a reduction of the system of boundary integral equations for a finite structure. Thus, the above example validates the formulation of equations both for the finite structure and for the structure having an infinitely long element. However, the energy calculations part of the solution by boundary equations cannot be checked by comparison with a finite element solution by ANSYS because the latter does not possess facilities for wave propagation analysis. To verify the validity of energy flow calculations, a spectral element method (see Doyle 1997) has been applied for calculating energy flows in a structure shown in Fig. 1b (see Part I). Its parameters are kept the same as listed above, but the length of the third element is taken to be infinitely large. No energy dissipation and no terminal points have been taken into account. The structure has been excited at the middle of the first element by a transverse driving force of amplitude 10 N. Structural intensities calculated by the boundary integral equation method at the interfaces between subsystems have been exactly the same as those obtained via the spectral element method. Thus, the suggested boundary integral formulation is proved to be valid also for calculations of structural intensities.

Analysis of wave propagation in tubular beams may only be adequately performed within the framework of the elementary theory of beams formulated by differential equations (2)–(3) from Part I up to a certain threshold frequency; the theory is applicable if the free wavelength is markedly larger than the diameter of the tube. Thus, it is necessary to estimate wavelength to diameter ratio for both flexural and longitudinal waves in the infinitely long element of the structure. In Fig. 2, the dependence of the nondimensional parameters $\frac{L_{\text{bending}}}{d_3}$ and $\frac{L_{\text{longit}}}{d_3}$ upon frequency in Hz is plotted. As follows from this graph, the elementary beam theory may reliably be used at least up to 400 Hz.

## 3
## Optimization, results and discussion

The problem of optimization has been formulated for a structure as shown in Fig. 1b (see Part I). Unlike the cases discussed earlier, the energy dissipation within the material of a structure has been included in our consideration. Specifically, the simple model of a frequency-independent loss factor has been adopted for all subsystems, i.e. $\eta_{wk}\omega = \eta_{uk}\omega = 10^{-4}$, $k = 1, 2, \ldots, 6$. The transverse driving force is applied at the middle of the first beam element and its amplitude is taken as uniformly distributed in the given frequency range. For definiteness, the amplitude of force is specified as 10 N and its phase is put to zero. Apparently, excitation conditions may include several other transverse and longitudinal driving forces with phases shifted from the first one. There is a wide variety of their possible combinations, but analysis of vibrations when several driving forces are applied to the structure lies beyond the scope of the present paper. It is more instructive to look into the possibilities of an active control of energy flows within the optimization framework that is possible by use of the suggested methodology. Thus, the last example of optimization to be given in this section is relevant to the case when the amplitude of a control force is chosen as a design variable.

A set of four terminal points is chosen as shown in Fig. 1b (see Part I) . The first terminal point coincides with the excitation point, and it has a mass of $M_1 = 2.5$ kg with no added stiffness and no damping. This terminal point in a real pipeline models a pump (a source of energy) which generates vibrations of the

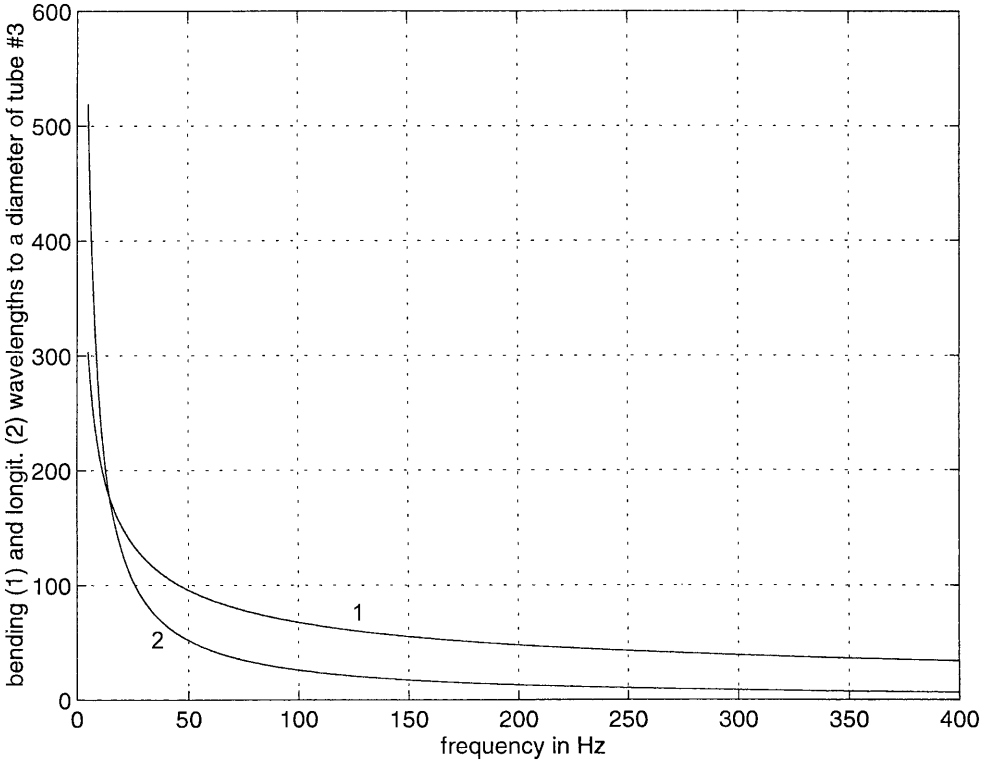


**Fig. 2** Nondimensional free wavelength parameters $\frac{L_{\text{bending}}}{d_3}$ (curve 1) and $\frac{L_{\text{longit}}}{d_3}$ (curve 2) versus frequency

whole structure. The second terminal point (an intermediate support of the pipeline) in the initial design is placed 30 cm to the right from the first one; its parameters are $M_2 = 1.5\,\text{kg}$, $K_2 = 3 \times 10^8\,\text{N/m}$ and internal loss factor is $\omega C_2 = 0.01 K_2$. The third terminal point is placed at the substructure (beam element) III in a distance of 3 m from its interface with the substructure II. This terminal point models a support of the third tubular element, and its parameters are $M_3 = 1.5\,\text{kg}$, $K_3 = 3 \times 10^8\,\text{N/m}$, $\omega C_3 = 0.01 K_3$. Similarly to those of the first terminal point, these parameters are not subjected to optimization. The fourth terminal point is placed between the interface of the second and the third beam elements and the terminal point 3. The parameters of this terminal point 4 are subjected to optimization.

An objective function is selected as the structural intensity measured at the distance of 5 m from the interface between substructures 2 and 3. As is seen in Fig. 1b, this control point is situated sufficiently far both from the excitation zone and from the introduced terminal points. Thus, it is reasonable to consider the structural intensity at this cross-section as an amount of vibration energy, which may produce undesirable noise emission from an "outer" part of the pipeline. The structural intensity at the control cross-section should be minimized for the frequency range from 40 to 100 Hz. This comparatively narrow frequency band is chosen for optimization of the structural performance since a low-frequency noise is most difficult to be suppressed by conventional means (see Norton 1986; Fuller *et al.* 1997). The structural intensity is calculated by a discrete counterpart of formula (7) in Part I,

$$\Theta = \sum_{k=1}^{60} N(\omega_k) \Delta\omega\,, \tag{1}$$

with an integration step of 1 Hz in the frequency domain, i.e. $\Delta\omega = 2\pi\,1/\text{s}$. This formulation of an objective function is approximate in the sense that it is related to sampling of the forced response of a structure with this accuracy. In principle, the convergence of this objective function to a certain value should be investigated when a number of sampling points is varied. However, just as in structural acoustics (see, e.g. Christensen *et al.* 1998) it is possible to restrict optimization of a structural response by a set of "master" frequencies. In the subsequent analysis, the latter approach is adopted.

### 3.1 Analysis of the initial design

In order to enable a good understanding of energy transmission mechanisms at the set of specified "master" frequencies, the behaviour of the system in its "initial design" is compared with the behaviour of the system when its terminal points are removed one by one. Some results of this comparison are illustrated in Fig. 3. In particular,

in Fig. 3a curve 1 presents the dependence of the power outflow $N_{\text{out}}$ $\left[\frac{\text{Nm}}{\text{s}}\right]$ at the control cross-section upon the excitation frequency when the system has no terminal points except for the first one. Curve 2 is plotted for the case, when only the terminal point 3 is added and curve 3 is plotted for the case when the terminal points 2 and 3 are added. As is seen, power outflow at the frequency of approximately 52.5 Hz is maximal in all three cases. Excitation of the structure at this frequency is associated with resonant behaviour of a concentrated mass. To explain this phenomenon, it is convenient to return to vibrations of a structure bearing only a concentrated mass (curve 1). Although the structure is infinitely long, the trapped mode effect (the strong localization of vibrations nearby the inhomogeneity) is produced by the presence of this mass. Since the driving force is applied directly at the mass, the power input into the pipeline also reaches its maximum at this frequency. As a very rough estimation of the value of this trapped mode resonant frequency, one may calculate the natural frequency of a single degree of freedom system composed as a simply supported weightless beam element 1 bearing the given concentrated mass. If the terminal point 3 is added, then the localization phenomenon becomes even more pronounced at the vicinity of the first trapped mode resonant frequency, see curve 2. In addition, a second peak of smaller magnitude is seen on this curve. This peak could be identified also as a resonant response of an inhomogeneous structure consisting of three beam elements. However, if one more terminal point (2) is added, then the energy transmission through the control cross-section is reduced, as is shown by curve 3, but it is still larger than in the case where the pipeline has no attachments. This is explained by the decrease in the amplitude of vibrations of the structure at the excitation point due to the relatively close location of a rather stiff terminal point 2.

These results show that addition/removal of terminal points may significantly change the energy consumption of the modelled system. In Fig. 3b, a radiation efficiency of travelling waves calculated as $N_{\text{out}}^{\text{bending}}/N_{\text{input}}+ N_{\text{out}}^{\text{longit}}/ N_{\text{input}}$ is plotted versus the excitation frequency for the same three cases. This graph clearly shows that in the specified frequency range practically the entire power input is transmitted through the structure with the selected parameters of terminal points. To compare contributions of bending waves and longitudinal waves, in Fig. 3c, the radiation efficiency of bending waves versus frequency is shown for the third element of the pipeline, where the control cross-section is positioned. Two conclusions follow from these graphs: (i) in this frequency range the vibration energy is conveyed mostly by bending waves, (ii) the radiation efficiency is very close to 1, so it is possible to formulate an objective function for the optimization procedure as the power input into the system.

Analysis of power flows between subsystems in the initial design is also performed in the selected frequency range. For the given excitation conditions, i.e. when a single transverse driving force acts at the first element, a power flow from the first element of the pipeline

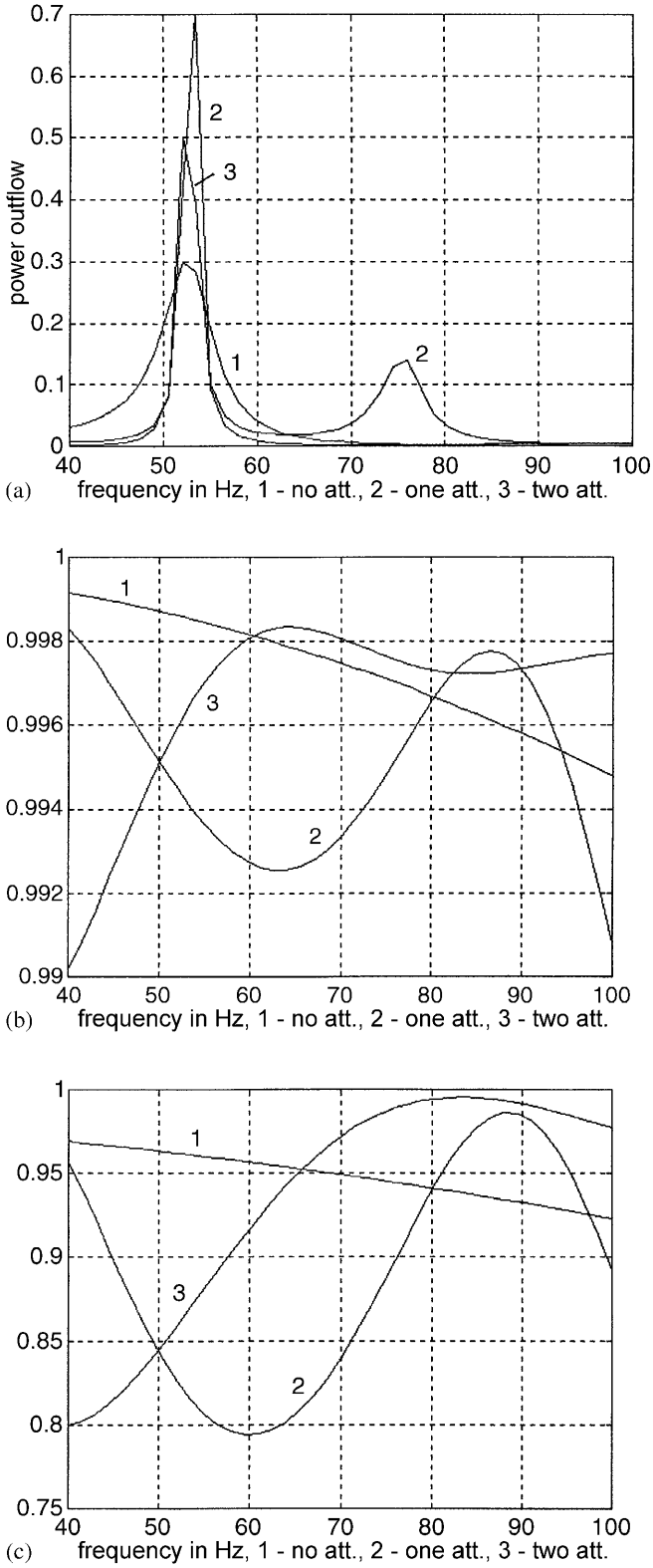


**Fig. 3** Comparison of energy flow characteristics for three configurations of the structure. (a) Power outflow at the control cross-section, (b) radiation efficiency of all travelling waves, (c) radiation efficiency of flexural waves

to the second one versus excitation frequency is shown in Fig. 4a. For convenience, the power flow is scaled to the energy input into the system. Curve 1 presents an overall power flow $N_{\text{out}}^{\text{bending}}/N_{\text{input}} + N_{\text{out}}^{\text{longit}}/N_{\text{input}}$. As has already been discussed, this quantity is fairly close to unity in the whole frequency range. Curve 2 shows the power flow carried by the longitudinal waves, $N_{\text{out}}^{\text{longit}}/N_{\text{input}}$ and it is negative whereas the power flow carried by the flexural waves $N_{\text{out}}^{\text{bending}}/N_{\text{input}}$ exceeds unity, as presented by curve 3. These results are explained by phenomena of energy exchanges between subsystems, namely, the energy of longitudinal waves in the second element is supplied by energy of flexural waves. In Fig. 4b, the similar graphs are presented for the energy flow to the third element. The overall energy flow $N_{\text{out}}^{\text{bending}}/N_{\text{input}} + N_{\text{out}}^{\text{longit}}/N_{\text{input}}$ is again slightly less than unity (due to the internal dissipation) as shown by curve 1. However, unlike partial energy flows in the second element, both quantities $N_{\text{out}}^{\text{bending}}/N_{\text{input}}$ (shown by curve 2) and $N_{\text{out}}^{\text{longit}}/N_{\text{input}}$ (shown by curve 3) are positive and their values agree with those presented in Fig. 3. It is clear that the distribution of the energy between longitudinal and flexural waves set up at the junction between the second and the third beam elements is preserved while the waves propagate along the third element and reach the control cross-section. We shall not pursue this aspect of analysis any further and now proceed to optimization of the structural performance.

### 3.2
### Parametric optimization

A parametric study of the influence of design parameters on the objective function has been carried out instead of using some standard optimization software. This decision was made due to a complex behaviour of the objective function in the specified frequency range. It

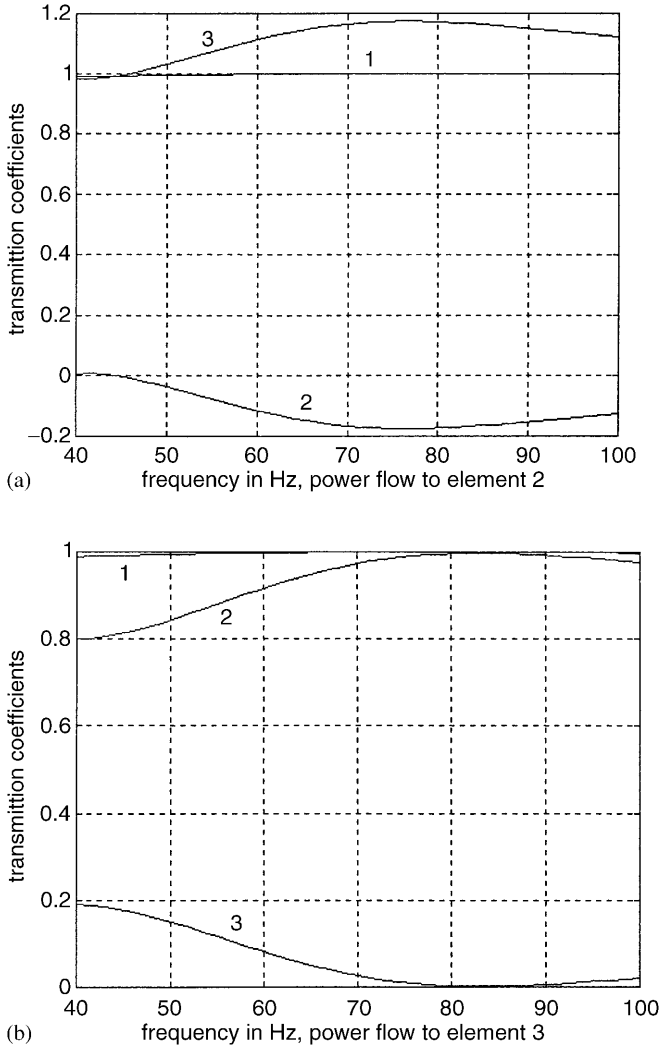


**Fig. 4** Energy flows between substructures. (a) Energy flow to the second beam element, (b) energy flow to the third beam element

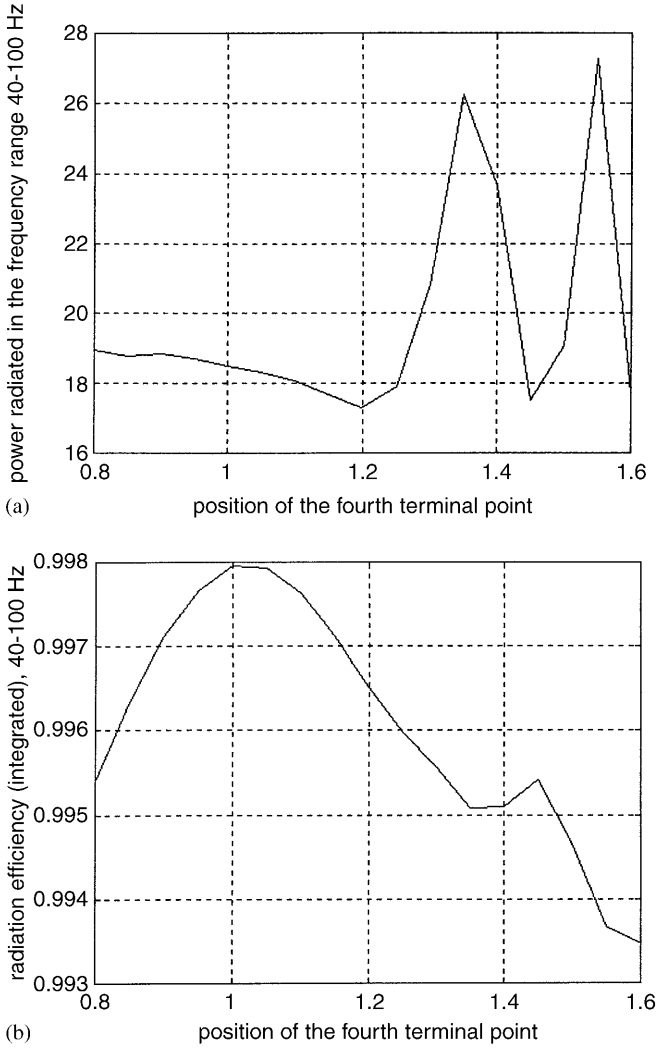


**Fig. 5** Optimization of positioning of the fourth terminal point (the first example). (a) Power outflow at the control cross-section, (b) radiation efficiency of all travelling waves

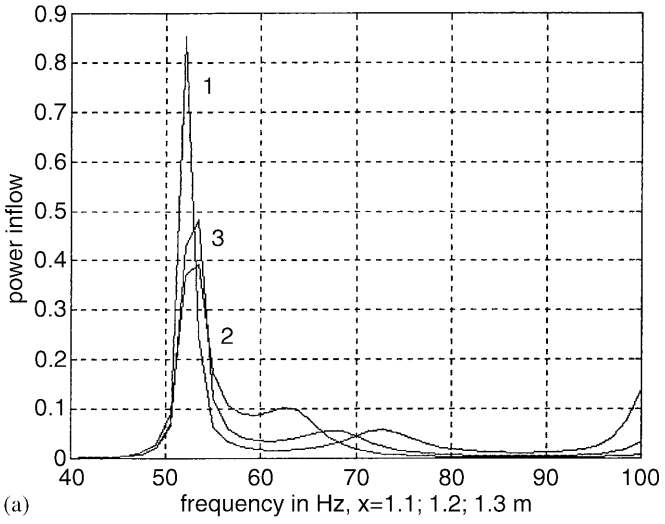


(a)

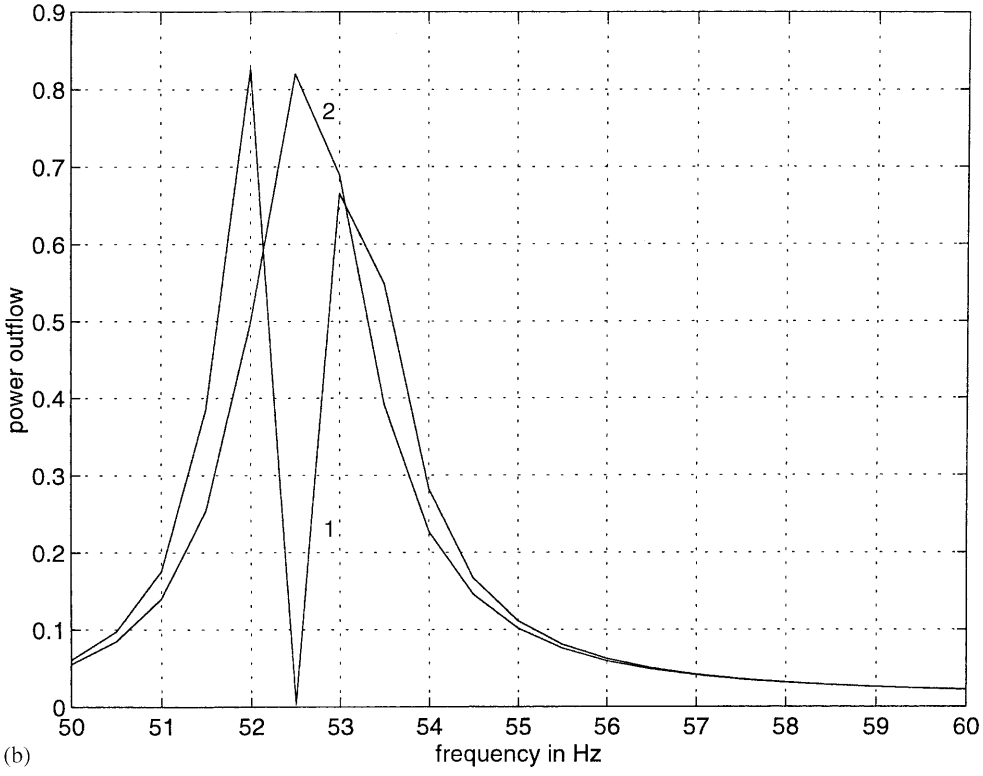


(b)

**Fig. 6** Energy flow characteristics of a structure. (a) Power input for three positions of the fourth terminal point: $x = 1.1$ m curve 1; $x = 1.2$ m curve 2; $x = 1.3$ m curve 3; (b) power outflow in a system with a dynamic absorber, curve 1 and without a dynamic absorber, curve 2

should also be pointed out that a parametric study provides a better understanding of the roles of the parameters of design in the physical process of transmission of power in the considered system. On the other hand, even if a moderate number of parameters of design is selected (as is done in the present paper), then it presents some difficulties to find the most representative cases of a parametric study. Thus, a few examples tackled in this subsection are aimed to provide the reader with some initial understanding of possible roles of various design variables, rather than to serve as a basis for any general conclusions concerning strategy of power flow optimization.

The optimization procedure has been started with mass, stiffness and damping parameters of terminal points 2, 3 and 4 fixed as they are given in the previous subsection. The positions of the second and the third terminal point have also been fixed as indicated there. Then the only design parameter that has been variable is the position of the fourth terminal point. The step in

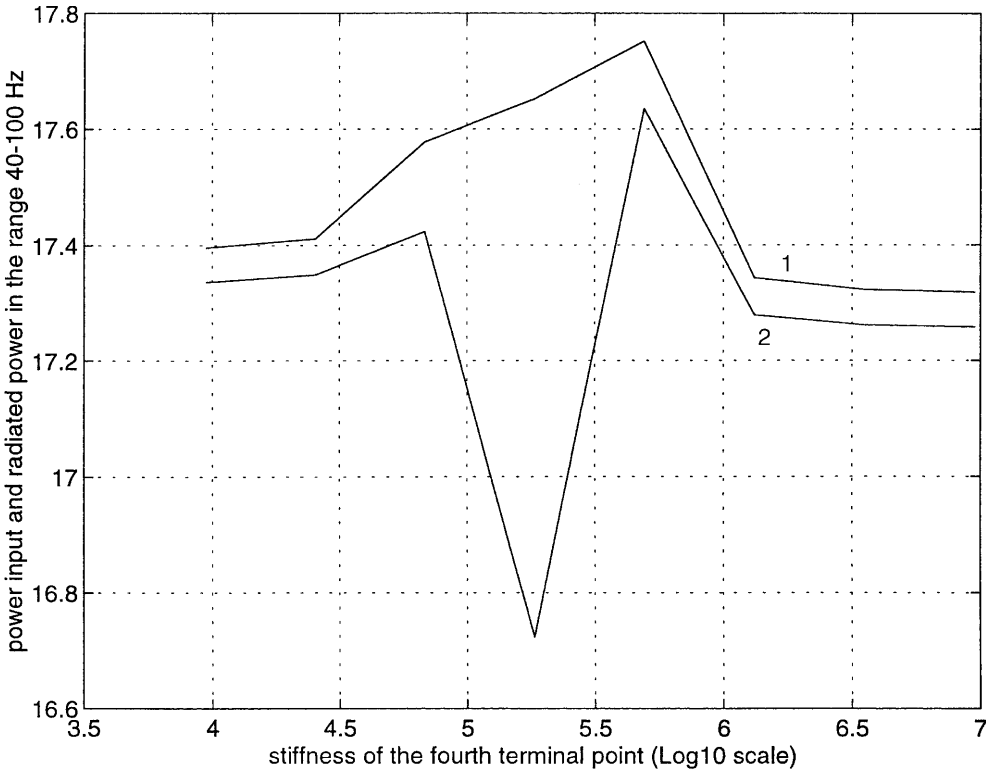


**Fig. 7** Dependence of power input (curve 1) and power output (curve 2) upon the stiffness of the fourth terminal point

changing co-ordinate of this terminal point has been chosen as 0.05 m and a simple constraint condition has been imposed to ensure that the terminal point cannot get closer than 10 cm to both the junction point and the terminal point 3, see Fig. 1b. For each configuration of the system, the power input and radiation efficiency coefficient have been computed for the whole frequency range with a step of 1 Hz. In Fig. 5a, the objective function (1) is plotted versus the co-ordinate of the fourth terminal point (the design variable). It is clearly seen that the power flow attains minimum value in $x = 1.2$ m. It should also be pointed out that the objective function oscillates when the design variable exceeds this value. The energy outflow is approximately the same when $x = 1.45$ m and when $x = 1.2$ m. However, the sensitivity of the objective function to changes of the design variable is larger in the former case than in the latter one. Thus, the optimal design location of the terminal point 4 should be selected as $x = 1.2$ m. In Fig. 5b, for the whole frequency range 40–100 Hz the radiation efficiency calculated is plotted (to different scale) versus the co-ordinate of this terminal point. It is clearly seen that the radiation efficiency is quite insensitive to the selected design variable and this characteristic of a structural performance cannot therefore serve as a reliable objective function for an optimization procedure. The results illustrated by Fig. 5 give a "global picture" of the structural behaviour in a given frequency range. A more detailed "local picture", i.e. the dependence of the energy input upon a frequency at three steps of optimization (i.e. for three positions of the terminal point) is presented in Fig. 6a. The principal contribution to the structural intensity is made by vibrations at the trapped mode resonant frequency, i.e. around 52.5 Hz. The dependence of the power outflow upon frequency in each of the cases is similar to the dependence of the power inflow since almost the whole input power is transmitted through the structure for the selected set of parameters.

As can be seen in Fig. 6a, the largest contribution to the input and the output power occurs at the resonant frequency related to a trapped mode generated by the concentrated mass at the terminal point 1. If an optimization problem is posed to minimise the output power only at this specific frequency, then to suppress resonant effects a dynamic absorber of vibrations may be effectively used. Such an absorber is modelled as a one-degree-of-freedom linear oscillator attached to the concentrated mass at the terminal point 1. Then (9) in Part I is formulated as

$$\left[-\omega^2 M_1 - K_0 \frac{\omega^2 + \frac{i\omega C_0}{K_0}}{\omega^2 - \Omega^2 + \frac{i\omega C_0}{K_0}} - i\omega C_0\right] v_1 = \Phi_1 \,. \qquad (2)$$

In (2) $\Omega = \sqrt{\frac{K_0}{M_0}}$ is the natural frequency of the absorber. The absorber's stiffness, mass and damping parameters are chosen to tune its resonant frequency to the trapped mode frequency of 52.5 Hz. They are

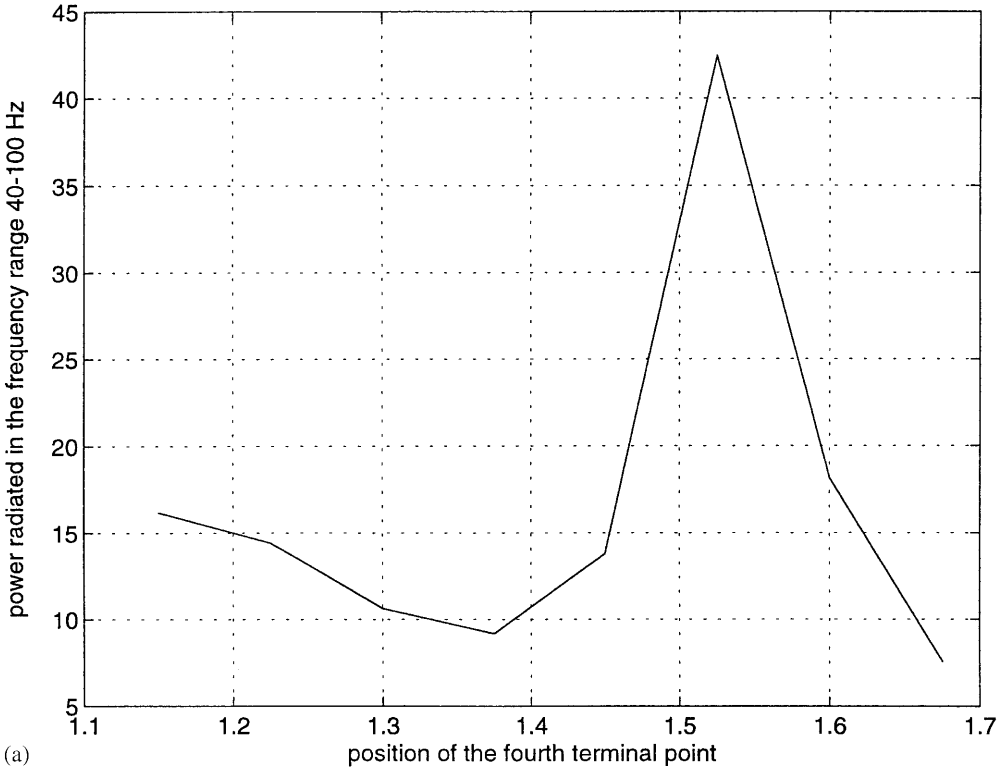


(a)

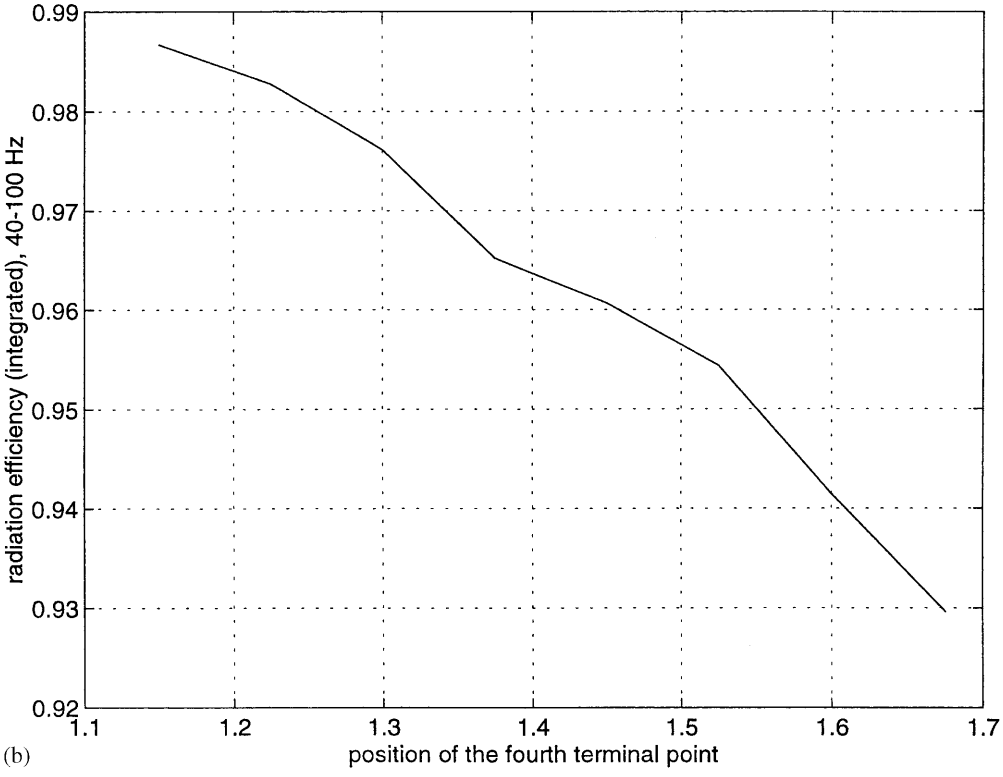


(b)

**Fig. 8** Optimization of positioning of the fourth terminal point (the second example). (a) Power outflow at the control cross-section, (b) radiation efficiency of all travelling waves

$K_0 = 10^3$ N/m, $M_0 = 9.2$ g, and $\Omega C_0 = 0.001 K_0$, respectively. The fourth terminal point is placed at $x = 1.1$ m. The dependence of the energy output upon a frequency is presented in Fig. 6b for the frequency range 50–60 Hz. As is clearly seen, the dynamic absorber is efficient only "locally" at the resonant frequency where the en-

ergy output drops practically to zero. At all other frequencies it does not produce any effect on the energy output. Therefore, the "global" role of a dynamic absorber in minimization of the objective function (1) in the whole given frequency range is insignificant and the further analysis is performed for a structure without absorbers.

After the optimal position of the fourth terminal point has been located, a similar parametric study is continued into the roles of stiffness, mass and damping parameters of a substructure connected with a "host" structure at this terminal point. In Fig. 7, the dependence of the power input (curve 1) and of a power transmitted through the control point (curve 2) upon stiffness of the fourth terminal substructure is presented. As is seen, both these characteristics are rather insensitive to variations in stiffness of this terminal substructure. There is only a rather small range around a value of $K_4 = 3 \times 10^5$ N/m where an increase in input power is associated with a decrease in radiated power. The role of an attached mass has also appeared to be insignificant. As it varies from 0 to 10 kg, it does not influence values of the input and the output power. The role of damping parameter is trivial: it influences only the transmission coefficient but not the power input into the system. Summing up the investigation into optimization of structural performance by varying parameters of the substructure at the terminal point 4 (see Figs. 5–7) it is concluded that by proper choice of design parameters, a value of the objective function may be reduced by about 10–15 % from its value for the initial design.

In the considered optimization example, a pipeline supported by comparatively stiff terminal points is modelled. The stiffness parameters of all supports are of the order of magnitude relevant to an axial stiffness of steel rods with a length of about 10 cm and a cross-sectional area of about 1 $cm^2$. It may be called an in-plane positioning of the pipelines supports since these rods are put in the plane where motions of the structure occur (as shown in Fig. 1b). The same rods may also be used to fix the pipeline in such a way that they experience a bending deformation. This is an "out-of-plane" (with respect to the plane in Fig. 1) positioning of the supports. Then the stiffness parameters of all the terminal points should be reduced about 1000 times to become $K_j = 3 \times 10^5$ N/m, $j = 1, 2, 3, 4$. This scaling factor is the ratio between axial and bending stiffness of these supports. As shown in Fig. 7, this particular value of the stiffness of the fourth terminal point would imply some decrease in the transmission coefficient. The internal loss factor at all terminal points is chosen to be the same as before, i.e. $\omega C_j = 0.01 K_j$, $j = 1, 2, 3, 4$. This assumption matches the one adopted for beam elements that an internal loss factor in bending vibrations of a pipeline is the same as in its longitudinal vibrations. An objective function is selected to have the form (1) and optimization is performed for the same frequency range as in the previous case. The results of an initial design analysis of a pipeline

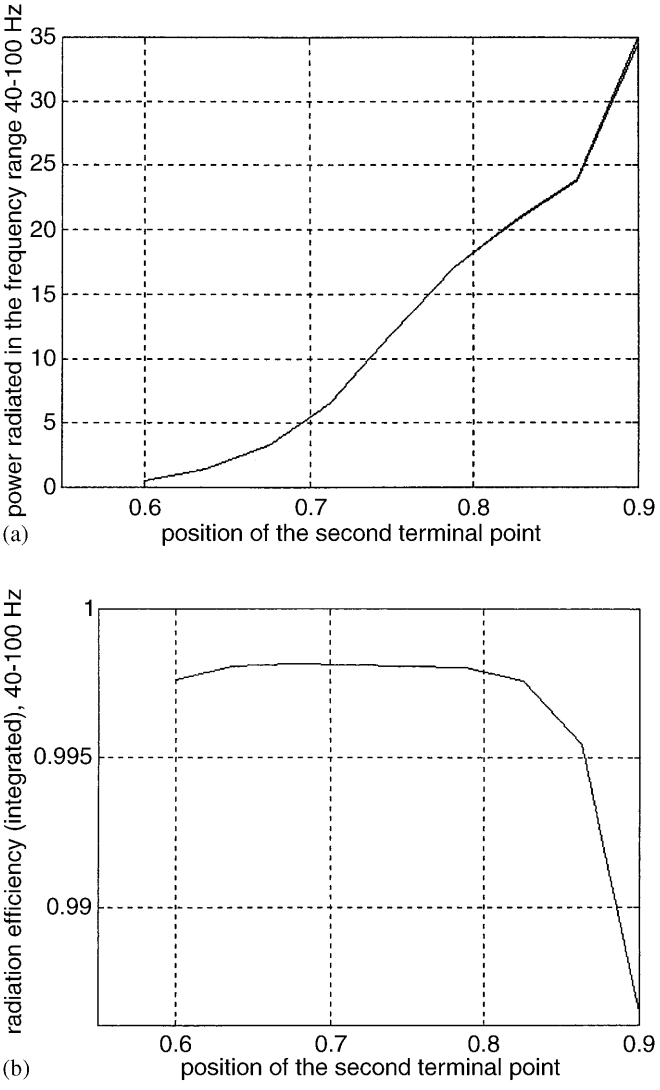


**Fig. 9** Optimization of positioning of the second terminal point. (a) Power outflow at the control cross-section, (b) radiation efficiency of all travelling waves

with "out-of-plane" or "bending" supports are quite similar to those illustrated in Fig. 3 and not displayed here. Similarly to the case of "axial" or "in-plane" supports, only one design parameter is variable that is the position of the fourth terminal point. For each configuration of the system, the power input and radiation efficiency coefficient have been computed for the whole frequency range with a step of 1 Hz. In Fig. 8a, the objective function (1) is plotted versus the co-ordinate of the fourth terminal point (a design variable). It is clearly seen that the power flow is minimized, when $x = 1.38$ m. This result is rather similar to what has been obtained for "out-of-plane" or "bending" supports at terminal points, see Fig. 5a. However, the value of radiated power is significantly reduced and as shown in Fig. 8b, the radiation efficiency is lower than in the previous case.

Another possibility of control is relevant to variation of parameters of the terminal point 2 (the one located

next to the excitation point). To perform a study of their roles, the fourth terminal point is placed at $x = 1.2$ m and all other parameters of the pipeline are kept as specified in Sect. 2 for the first example of optimization (i.e. "in-plane" connection at terminal points is considered). In Fig. 9a, the dependence of the power flow on the position of the second terminal point is shown. As is seen, it is more efficient to control the energy output by letting the second terminal point tend to the excitation point, than to change the location of the fourth terminal point. Apparently, the best performance of the structure could be achieved when the terminal point merges the excitation point. Physically, it is explained simply by a significant reduction of the amplitude of vibrations at the excitation point produced by a presence of the stiffener. This result is well-known in many practical applications as suppression of vibrations at the source. However, a constraint similar to that in the previous case has been imposed to prevent the second terminal point to be positioned closer than 10 cm to the point of excitation. In Fig. 9a it is seen that a minimum of power transmission is reached just when a terminal point is placed at this distance from the source (i.e. as near as permitted). In Fig. 9b, the efficiency of radiation is plotted versus the position of the terminal point, and it is clear that just in all the previous cases, this quantity is insensitive to variations in design parameters.

In Fig. 10, the dependence of an energy flow through a control cross-section of an optimized structure (a structure with the second terminal point positioned 10 cm from an excitation point) is plotted in a broad frequency range (0–200 Hz). Simultaneously, the dependence of an energy flow upon the frequency for the initial design (a structure with the second terminal point positioned in 30 cm from an excitation point) is also presented. Optimal location of the second terminal point improves a performance of the structure in a broader frequency range than the range specified for the optimization process.

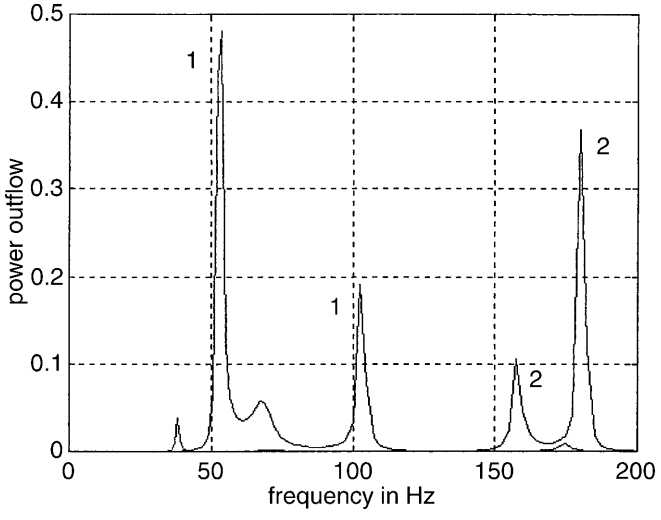


**Fig. 10** Power outflow at the control cross-section (1 – initial design, 2 – optimized structure)

However, the overall decrease in structural intensity in the frequency range 0–200 Hz is not as large as in the range 40–100 Hz. As is seen from the graph, there are two peaks of energy outflow of an optimized structure at about 157 Hz and 178 Hz, whereas the initial design has peaks of larger magnitude at the frequencies of 52.5 Hz and 104 Hz. Physically, a shift of "resonant" (in the sense of maximum energy transmission) frequencies towards larger values is explained by an increase in the stiffness of the whole structure generated by relocation of the second terminal point.

To conclude our investigation into the dynamics of the model structure, the possibility of an active control of power outflow by means of a "secondary" control force is explored. This transverse force is applied at the middle of the second beam element. For simplicity, an active control is restricted by a variation in the amplitude of

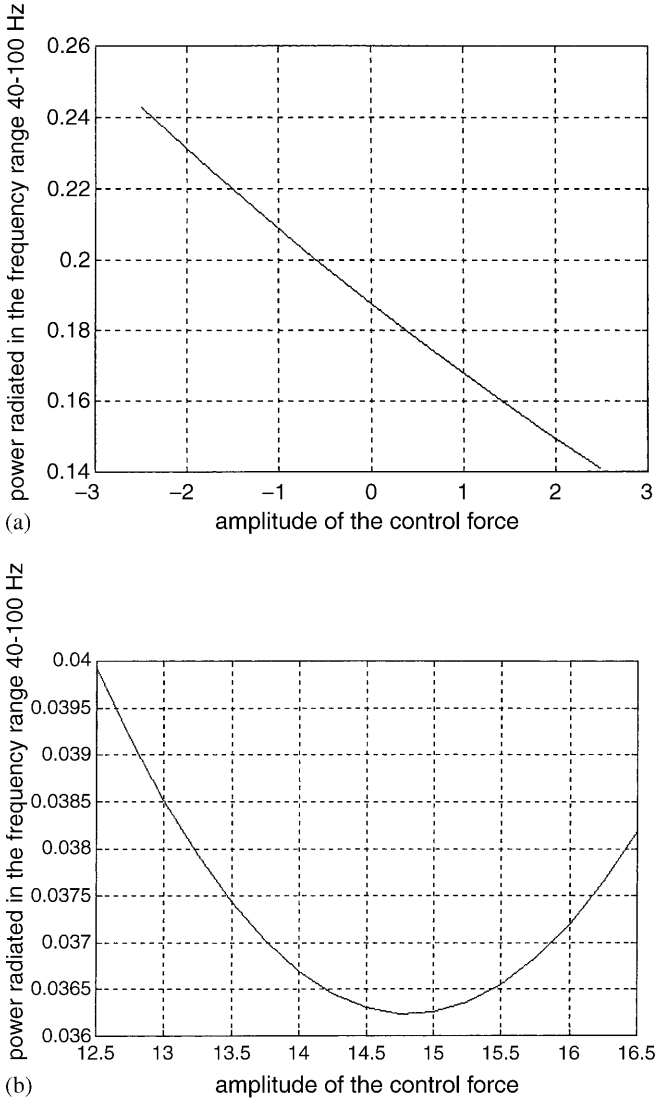


**Fig. 11** Power outflow control by "secondary" source. (a) Power outflow at the control cross-section for small amplitudes of a control force, (b) minimization of the power outflow at the control cross-section by a control force

this secondary source, whereas it acts in phase with the primary one. Then negative values of its amplitude are relevant to a force shifted in $\pi$ radians from the driving force. The technique used in this paper for analysing forced vibrations and energy flows may easily be adopted to take into account possible phase shifts between active and secondary sources. However, more detailed inspection into active control of vibrations of pipe systems (see Norton 1986; Fuller *et al.* 1997) lies beyond the scope of the present paper. In Fig. 11a, the influence of a control force of fairly small amplitude on the power outflow through the control cross-section is illustrated. The presence of the secondary source acting in phase with the primary one reduces energy outflow. Apparently, from a practical viewpoint the amplitude of a control force should be much less than the amplitude of a driving force. However, as suggested by the results shown in Fig. 11a interaction of two in-phase forces significantly reduces the energy outflow. This conclusion is supported by the graph in Fig. 11b, which in fact is an extension of Fig. 11 a towards large amplitudes of the "secondary" force. As it follows from this graph, the optimal value of the secondary force is very large (1.48 times larger than an amplitude of the primary force), but it gives a very large reduction in power transmission through the control cross-section (almost 5 times).

## 4 Conclusions

An investigation of in-plane coupled flexural and longitudinal vibrations of a planar structure composed by tubular elements of both a finite and an infinite length is presented. The mechanical system is modelled by a set of coupled subsystems introduced as elastic wave-guides carrying flexural or longitudinal waves. The purpose of the study is an optimization of energy flows from a source to a remote zone of a structure for a given frequency range and given excitation conditions by means of varying the location, stiffness, damping and mass parameters of the attached terminal points. A boundary integral equation method is used to set up a system of governing equations describing forced stationary vibrations of the structure. Validity of this problem formulation is checked via comparison of numerical results obtained by usage of the boundary integral method, the finite element method and the spectral element method. The parametric study of vibrations of a model structure has shown that at the specified low-frequency range, the structural intensity (the energy flow) at the remote part of a structure is very close to the power input. Thus, for the sets of parameters considered in this paper, the radiation efficiency coefficient is a very robust characteristic of a vibrating structure and it slightly depends upon selected design variables. The algorithm based on use of boundary equations is also used to analyse energy flows between subsystems and to compare contributions to the structural intensity from flexural and longitudinal waves.

The objective function is selected as the power input into the system and the optimization strategy is set up as reduction of the power input because it simultaneously gives the minimization of an energy outflow. Presence of several terminal points strongly affects the above objective function. Specifically, the power input into a structure with terminal points at a certain rather narrow frequency range is much higher than that for a structure with no terminal points due to resonant mode trapping. Several case studies of optimization are performed to show that a proper choice of positions of the terminal points (which are the most influential design variables) may significantly improve structural performance in a broad frequency range. It is also shown that the objective function is not equally sensitive to all considered design parameters. In particular, the sensitivity with respect to mass characteristics of terminal points (at least, within their variability range considered in the paper) is much lower than to their location parameters. It is found that a dynamic absorber capable to suppress vibrations at the given individual frequency is not an efficient tool to reduce the energy outflow in a broad frequency range.

Finally, the formulation of a problem in optimization is extended to include amplitudes of "complementary" driving forces in the set of design variables, i.e. an active control of structural intensities is considered, and a significant effect of such a control strategy is shown.

## References


Swanson Analysis Systems Inc. 1992: *ANSYS user's manual for revision 5.0*

Christensen, S.T.; Sorokin, S.V.; Olhoff N. 1998: On analysis and optimization in structural acoustics. Part II: exemplifications for axisymmetric structures. *Struct. Optim.* **16**, 83–95

Doyle, J.F. 1997: *Wave propagation in structures*. Berlin, Heidelberg, New York: Springer

Fuller, C.R.; Fahy, F.J. 1982: Characteristics of wave propagation and energy distribution in cylindrical elastic shells filled with fluid. *J. Sound & Vib.* **81**, 501–518

Fuller, C.R.; Elliott, S.J.; Nelson, P.A. 1997: *Active control of vibration*. London: Academic Press

Lyon, R.H. 1975: *Statistical energy analysis of dynamical systems: theory and applications*. Cambridge, MA: MIT Press

Meirovitch, L. 1990: *Dynamics and control of structures*. New York: John Wiley & Sons

Norton, M.P. 1986: *Fundamentals of noise and vibration analysis for engineers*. Cambridge, UK: Cambridge University Press

Pavic, G. 1993: Vibroacustical energy flow through straight pipes. *J. Sound & Vib.* **154**, 411–429

Petyt, M. 1990: *Introduction to finite element vibration analysis*. Cambridge, UK: Cambridge University Press

Ren and Beards (1995)]ReBe95 Ren, Y.; Beards, C.F. 1995: On substructure synthesis with FRF data. *J. Sound & Vib.* **185**, 845–866

Rozvany, G.I.N. 1976: *Optimal design of flexural systems*. Oxford: Pergamon Press

Shankar, K.; Keane, A.J. 1995a: A study of the vibrational energies of two coupled beams by finite element and Green function (receptance) methods. *J. Sound & Vib.* **181**, 801–838

Shankar, K.; Keane, A.J. 1995b: Energy flow predictions in a structure of rigidly joined beams using receptance theory. *J. Sound & Vib.* **185**, 867–890

Sorokin, S.V. 1993: Asymptotic analysis and numerical solution of the two-level boundary equations of a plane problem of stationary hydroelasticity. *J. Appl. Math. & Mech.* **57**, 105–115

Sorokin, S.V.; Nielsen, J.B.; Olhoff, N. 2001: Analysis and optimization of energy flows in structures composed of beam elements. Part I: problem formulation and solution technique. *Struct. Multidisc. Optim.* **22**, 3–11